CHEMISTRY
A EUROPEAN JOURNAL

DOI: 10.1002/chem.200801852

Spin Crossover in a Family of Iron(II) Complexes with Hexadentate ligands: Ligand Strain as a Factor Determining the Transition Temperature

Galina S. Matouzenko,*[a] Serguei A. Borshch,[a] Erwann Jeanneau,[b] and Mark B. Bushuev[c]

Abstract: This paper reports the synthesis of a family of mononuclear complexes $[Fe(L)]X_2$ ($X = BF_4$, PF_6, ClO_4) with hexadentate ligands L = Hpy-DAPP ({bis[*N*-(2-pyridylmethyl)-3-aminopropyl](2-pyridylmethyl)amine}), Hpy-EPPA ({[*N*-(2-pyridylmethyl)-3-aminopropyl][*N*-(2-pyridylmethyl)-2-aminoethyl](2-pyridylmethyl)amine}) and Hpy-DEPA ({bis[*N*-(2-pyridylmethyl)-2-aminoethyl](2-pyridylmethyl)amine}). The systematic change of the length of amino-aliphatic chains in these ligands results in chelate rings of different size: two six-membered rings for Hpy-DAPP, one five- and one six-membered rings for Hpy-EPPA, and two five-membered rings for Hpy-DEPA. The X-ray analysis of three low-spin complexes $[Fe(L)](BF_4)_2$ revealed similarities in their molecular and crystal structures. The magnetic measurements have shown that all synthesized complexes display spin-crossover behavior. The spin-transition temperature increases upon the change from six-membered to five-membered chelate rings, clearly demonstrating the role of the ligand strain. This effect does not depend on the nature of the counter ion. We discuss the structural features accountable for the strain effect on the spin-transition temperature.

Keywords: chelates · iron · magnetic properties · N ligands · spin crossover

Introduction

The engineering of spin-crossover systems presents an important area of research in molecular magnetism. A steady interest in spin-crossover phenomenon is conditioned by both theoretical aspects and potential applications of new materials in molecular electronics. After its discovery in the early 1930s,[1] the spin crossover has been extensively studied by a variety of physical methods and the results have been summarized in several reviews.[2–11] Potential use of spin-crossover systems for information storage[12,13] requires an abrupt spin transition with a relatively large thermal hysteresis, centered near to ambient temperature. However, it should be emphasized that despite the systematic efforts of chemists, our knowledge in the synthesis of spin-crossover compounds with predictable characteristics is rather limited. It is well known that proximity of the high-spin (HS) and low-spin (LS) electronic states is a prerequisite for the occurrence of a spin crossover. The energy gap between two states can be tuned in a relatively predictable fashion by variation of the ligand field force. However, the ligand field strength is not the only factor determining the spin-transition existence and character. The interplay of the spin-pairing energy and the ligand field strength is very sensitive to small structural perturbations in the metal environment. They may result from the existence of sterically demanding ligands, and/or from minor crystal-packing changes associated with the nature of the counter ions, or the presence of a solvent of crystallization. All these factors offer difficulties for the synthesis of new compounds with desirable magnetic properties. Many compounds reported in the literature illustrate this situation. Moreover, even more delicate features in the ligand, such as the number of chelate rings and/or replacement of five- to six-membered cycles can also affect the spin state of the resulting iron(II) complex. Recent examples clearly demonstrated that the chelate ring size could

[a] Dr. G. S. Matouzenko, Dr. S. A. Borshch
Laboratoire de Chimie (UMR CNRS and ENS-Lyon no.5182)
École Normale Supérieure de Lyon
46, allée d'Italie, 69364 Lyon cedex 07 (France)
Fax: (+33)47272-8860
E-mail: Galina.Matouzenko@ens-lyon.fr

[b] Dr. E. Jeanneau
Laboratoire des Multimatériaux et Interfaces (UMR CNRS no.5615)
Université Claude Bernard Lyon-1
69622 Villeurbanne cedex (France)

[c] Dr. M. B. Bushuev
Nikolaev Institute of Inorganic Chemistry
Siberian Branch of the Russian Academy of Sciences
3, Akad. Lavrentiev Av., Novosibirsk, 630090 (Russia)

strongly affect chemical and physical properties of coordination compounds. For example, significant chelate-ring-size effects have been found in the copper-dioxygen chemistry,[14,15] catechol dioxygenase reactivity of iron(III) compounds,[16] electrochemical properties of manganese(III) and (IV) complexes,[17] spectroscopic properties of nickel(II)[18] and cobalt(III) compounds.[19–21] Some attempts to consider the effect of chelate cycles size on the spin state of iron(II) have been done in the literature.[22–24] However, to our knowledge, there is no example in the literature of a series of similar compounds with successive changes in the size of chelate cycles, all of them manifesting a spin-crossover behavior.

It is well known that five-membered chelate rings are more strained than those that are six-membered. The conformational freedom of six-membered chelate rings has been found to be responsible for several polymorphic modifications for the same iron(II) spin-crossover complex[25] or to lead to order–disorder structural transitions in the coordination sphere of complex.[26,27] In this context, polydentate ligands capable of generating one or several six-membered chelate rings in coordination with iron(II), conveying a flexible coordination sphere, are of special interest. The synthesis of families of complexes with successive changes in the ligand structure should allow us to follow the influence of such modifications on the shape of spin transitions.

Recently, we have reported the synthesis of the mononuclear complex $[Fe^{II}(Hpy\text{-}DAPP)](BF_4)_2$ (**1a**) (Hpy-DAPP = {bis[*N*-(2-pyridylmethyl)-3-aminopropyl](2-pyridylmethyl)-amine}) with the hexadentate ligand (Scheme 1), capable of

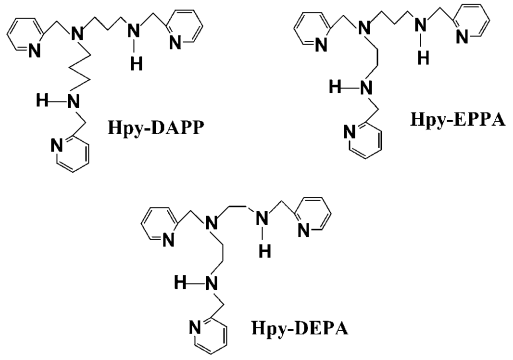

Scheme 1.

forming both five- and six-membered chelate rings.[27] To perform a systematic study of the strain effects on the spin transition characteristics, resulting from the chelate rings size, we obtained two new hexadentate ligands (Scheme 1) to make possible the synthesis of a family of mononuclear iron(II) complexes involving the chelate rings of different size. Moreover, to examine the dependence of found effects on the counter-ion nature as well, each complex was prepared with three different counter ions, namely tetrafluoroborate, hexafluoroborate and perchlorate. The X-ray analysis of three compounds $[Fe(L)](BF_4)_2$ reveals similar geometries for their $[FeN_6]$ coordination cores. All compounds exhibit spin-crossover behavior, established by the magnetic susceptibility measurements. The magnetic data clearly demonstrate the spin-crossover temperature dependence on the strain effects, which result from the size of chelate rings. The successive reduction in size from six- to five-membered chelate ring leads to the rise of transition temperature in this family of compounds. The found dependence does not depend on the counter-ion nature. The observed effect will be discussed in terms of the continuous shape measures[28,29] of the $[FeN_6]$ coordination core.

Results

Syntheses: In addition to the previously reported hexadentate ligand Hpy-DAPP, we performed the syntheses of two new ligands Hpy-EPPA ({[*N*-(2-pyridylmethyl)-3-aminopropyl][*N*-(2-pyridylmethyl)-2-aminoethyl](2-pyridylmethyl)-amine}) and Hpy-DEPA ({bis[N-(2-pyridylmethyl)-2-aminoethyl](2-pyridylmethyl)amine}) (Scheme 1). With each ligand L, we synthesized three mononuclear complexes $[Fe(L)]X_2$ with the following counter ions X: BF_4 (**1a**, **2a**, and **3a** for the complexes with Hpy-DAPP, Hpy-EPPA, and Hpy-DEPA, respectively), PF_6 (**1b**, **2b**, and **3b**), and ClO_4 (**1c**, **2c**, and **3c**). The syntheses were carried out in mixed methanol/ethanol solvent systems using glovebox techniques. All products were isolated as well shaped crystals. The crystals used in the X-ray structure determinations were selected from the sample synthesized according the procedure described below.

Magnetic properties: Variable-temperature magnetic susceptibility data were collected in both cooling and warming modes in the range of 15–500 K. The data, bunched in three groups according to their counter ions, are presented as $\chi_M T$ versus T plots (Figure 1–3).

All studied complexes with the BF_4 counter ion display the spin-crossover behavior (Figure 1). The spin transition

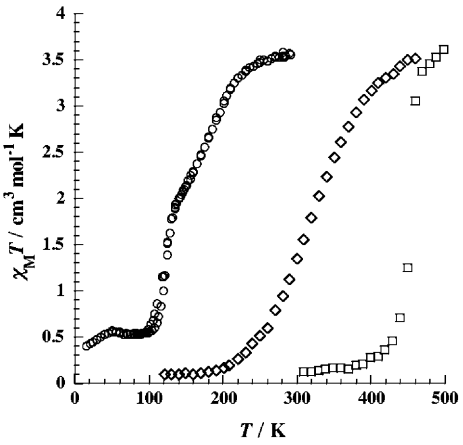

Figure 1. Thermal variation of $\chi_M T$ for $[Fe(Hpy\text{-}DAPP)](BF_4)_2$ (**1a**, ○), $[Fe(Hpy\text{-}EPPA)](BF_4)_2$ (**2a**, ◇), $[Fe(Hpy\text{-}DEPA)](BF_4)_2$ (**3a**, □).

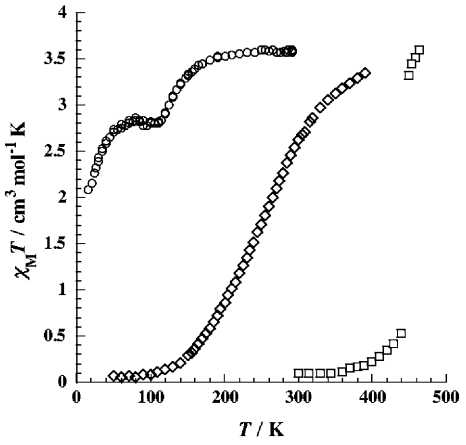

Figure 2. Thermal variation of $\chi_M T$ for [Fe(Hpy-DAPP)]$(PF_6)_2$ (**1b**, ○), [Fe(Hpy-EPPA)]$(PF_6)_2$ (**2b**, ◇), [Fe(Hpy-DEPA)]$(PF_6)_2$ (**3b**, □).

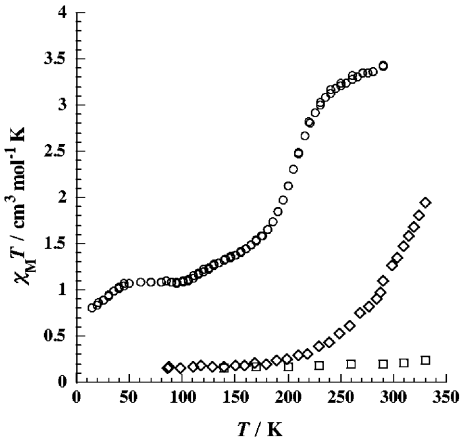

Figure 3. Thermal variation of $\chi_M T$ for [Fe(Hpy-DAPP)]$(ClO_4)_2$ (**1c**, ○), [Fe(Hpy-EPPA)]$(ClO_4)_2$ (**2c**, ◇), [Fe(Hpy-DEPA)]$(ClO_4)_2$ (**3c**, □).

for the complex **1a**[27] occurs in two steps separated by an inflexion point at 130 K at which 50% of complexes undergo a spin conversion. The high-temperature step centered at 181 K is gradual, whereas the low-temperature one displays a thermal hysteresis with two transition temperatures ($T_c\downarrow$ = 119 K and $T_c\uparrow$ = 123 K). The **2a** complex exhibits a gradual spin-crossover behavior with the high- and low-temperature $\chi_M T$ values (3.52 and 0.10 cm^3 mol^{-1} K, respectively) showing a complete spin change. The spin-transition temperature $T_{1/2}$ (temperature for which the HS fraction is equal to 0.5) is found at 320 K. The **3a** complex transits very abruptly, but without thermal hysteresis. The $T_{1/2}$ temperature (455 K) is a highest in this series.

The second group of compounds **1b**, **2b**, and **3b** encloses the PF_6 derivatives (Figure 2). The complex **1b** is in the HS state at room temperature. The $\chi_M T$ magnitude, equal to 3.59 cm^3 mol^{-1} K at 290 K, remains fairly constant with decreasing temperature until 150 K and then gradually decreases upon cooling to 2.78 cm^3 mol^{-1} K at 90 K. This decrease of the $\chi_M T$ value corresponds to a partial (≈23%) HS→LS conversion. Below 90 K, the $\chi_M T$ value slightly increases to 2.83 cm^3 mol^{-1} K at 80 K and then progressively decreases to 2.09 cm^3 mol^{-1} K at 15 K. The **2b** complex undergoes a gradual spin crossover. Between 100 and 400 K, the $\chi_M T$ value varies from 0.10 to 3.41 cm^3 mol^{-1} K indicating a quasi-complete spin transition. The spin-transition temperature $T_{1/2}$ is found close to 255 K. The **3b** complex is in the LS state at room temperature. The HS $\chi_M T$ value equal to 3.60 cm^3 mol^{-1} K is reached at 460 K. The spin-transition temperature $T_{1/2}$ is equal to 442 K. Despite the abrupt spin crossover, the hysteresis effect is absent.

The third group comprises the perchlorate complexes **1c**, **2c**, and **3c** (Figure 3). The **1c** complex exhibits a spin crossover behavior. At room temperature the magnitude of $\chi_M T$ (3.43 cm^3 mol^{-1} K) corresponds to a quintet spin state. This value gradually decreases upon cooling to 185 K and reaches 1.73 cm^3 mol^{-1} K, which indicates half of the iron(II) sites have undergone a spin transition. Below this temperature, the $\chi_M T$ value descends slowly to reach 1.10 cm^3 mol^{-1} K at 100 K, and then it remains fairly constant with decreasing temperature until 45 K. Further cooling to 15 K leads to the $\chi_M T$ value equal to 0.80 cm^3 mol^{-1} K. This weak paramagnetism can be related to a residual amount of the HS fraction (≈20%), probably due to the slow kinetics of HS→LS relaxation.[19] In the warming mode the same magnetic behavior as in the cooling one was observed. Because of potentially explosive properties of the perchlorate salts, the complexes **2c** and **3c** were heated to 330 K. For compound **2c**, the variation of $\chi_M T$ in the range of 85–330 K conforms to a partial (55%) spin conversion with $T_{1/2}$ equal to 320 K. The compound **3c** shows a weak increasing tendency for the $\chi_M T$ value up to 330 K, so the presence of spin crossover at higher temperatures can be expected.

Description of the structures: The structural studies have been performed for the complexes **2a** and **3a** with the BF_4 counter ion, in addition to the already described complex **1a** (Figure 4).[27] Single-crystal X-ray diffraction structures of **2a**

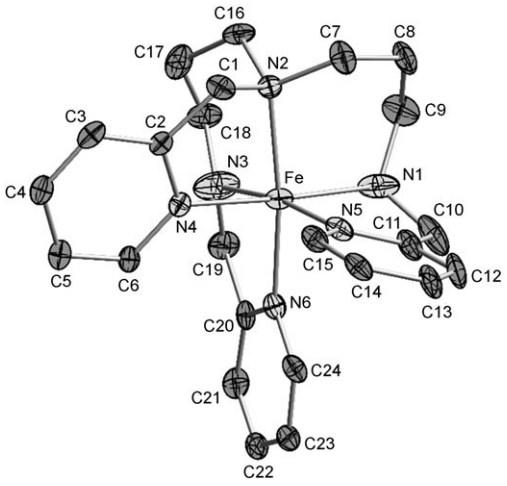

Figure 4. View of the [Fe(Hpy-DAPP)]$(BF_4)_2$ (**1a**) molecule at 90 K.[27] Ellipsoids enclose 30% probability. The counter-ions and hydrogen atoms have been omitted for clarity.

and **3a** were determined in the LS state at 150 K. All structures belong to the monoclinic $P2_1/c$ group with $Z=4$ (see Table 1 for further information about the unit cell). Perspective views of the **2a** and **3a** mononuclear complexes are presented in Figure 5 and 6. Selected bond lengths and angles are given in Table 2. In both compounds the octahedral coordination sphere of the iron(II) atom comprises three aliphatic and three aromatic-nitrogen atoms. In principle, a variety of isomers can exist, owing to the polydentate ligand coordination to the iron(II) atom. For example, three pyridine nitrogen atoms (or three aliphatic amino groups) can occupy facial or meridional positions in the $[FeN_6]$ octahedron. Moreover, an octahedral coordination leads to a possible existence of two stereoisomers (Δ or Λ configurations). In both **2a** and **3a** compounds the ligands adopt a similar *fac* configuration and the unit cell contains two pairs of symmetry-related left-handed and right-handed enantiomers. The hexadentate ligand coordinated to iron(II) produces one six-membered and four five-membered chelate rings in **2a**, whereas all five chelate rings are five-membered in **3a**.

Table 1. Crystallographic data for **2a** and **3a**.[a]

	2a	**3a**
formula	$C_{23}H_{30}N_6B_2F_8Fe$	$C_{22}H_{28}N_6B_2F_8Fe$
M	619.98	605.96
T [K]	150	150
system	monoclinic	monoclinic
space group	$P2_1/c$	$P2_1/c$
a [Å]	12.755(1)	11.963(1)
b [Å]	14.156(1)	15.107(1)
c [Å]	14.915(1)	14.518(1)
β [°]	106.375(2)	107.100(2)
V [Å^3]	2583.8(1)	2507.7(1)
ρ_{calcd} [g cm^{-3}]	1.594	1.605
Z	4	4
λ [Å]	0.71069	0.71069
$\mu(Mo_{K\alpha})$ [mm^{-1}]	0.668	0.686
$F(000)$	1272	1240
θ range [°]	1.7–27.8	1.8–27.9
independent reflns	6096	5969
reflns with $[I>2\sigma(I)]$	4362	4327
parameters	361	352
$R[F^2>2\sigma(F)^2]$	0.0765	0.0476
$wR_2(F^2)$	0.0833	0.0525

[a] Estimated standard deviations in the least significant digits are given in parentheses.

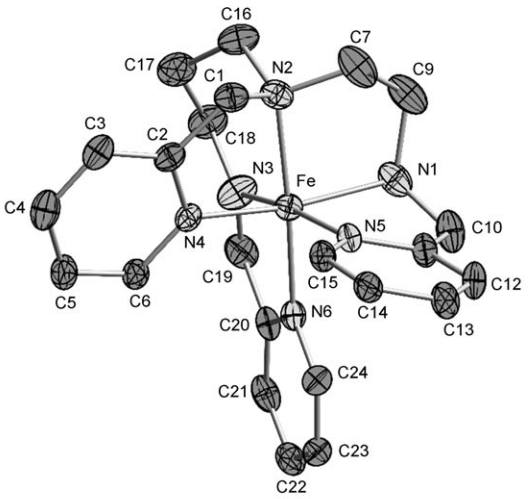

Figure 5. View of the $[Fe(Hpy\text{-}EPPA)](BF_4)_2$ (**2a**) molecule at 150 K. Ellipsoids enclose 30% probability. The counter-ions and hydrogen atoms have been omitted for clarity.

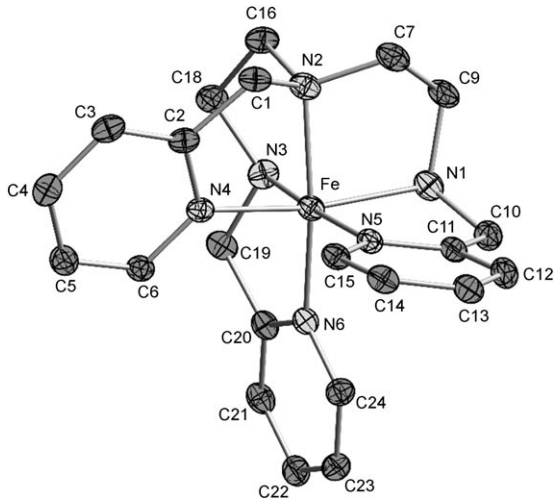

Figure 6. View of the $[Fe(Hpy\text{-}DEPA)](BF_4)_2$ (**3a**) molecule at 150 K. Ellipsoids enclose 30% probability. The counter-ions and hydrogen atoms have been omitted for clarity.

Table 2. Selected bond lengths [Å] and angles [deg] for **1a**,[27] **2a**, and **3a**.[a]

	1a	**2a**	**3a**
Fe1–N1	2.009(5)	2.020(3)	2.020(2)
Fe1–N2	2.128(4)	2.047(3)	2.004(2)
Fe1–N3	2.085(6)	1.969(4)	1.989(2)
Fe1–N4	2.049(4)	1.964(3)	1.973(2)
Fe1–N5	2.033(5)	1.999(3)	1.984(2)
Fe1–N6	2.061(4)	1.997(3)	1.974(2)
N1–Fe1–N2	94.4(2)	87.4(1)	86.5(1)
N1–Fe1–N3	97.5(3)	95.7(2)	91.9(1)
N1–Fe1–N4	175.1(2)	168.8(1)	168.0(1)
N1–Fe1–N5	83.0(2)	81.0(1)	82.3(1)
N1–Fe1–N6	90.4(2)	94.2(1)	94.7(1)
N2–Fe1–N3	94.5(2)	94.5(1)	84.7(1)
N2–Fe1–N4	81.4(2)	82.8(1)	82.9(1)
N2–Fe1–N5	94.7(2)	94.7(1)	95.9(1)
N2–Fe1–N6	172.4(2)	174.7(1)	168.2(1)
N3–Fe1–N4	85.3(3)	90.3(2)	92.8(1)
N3–Fe1–N5	170.7(2)	170.1(1)	174.0(1)
N3–Fe1–N6	79.0(2)	80.3(1)	83.6(1)
N4–Fe1–N5	94.9(2)	94.6(1)	93.1(1)
N4–Fe1–N6	94.1(2)	96.1(1)	96.9(1)
N5–Fe1–N6	91.7(2)	90.5(1)	95.9(1)

[a] Estimated standard deviations in the least significant digits are given in parentheses.

Low-spin 2a complex structure ($T=150$ K): The structural characteristics found for **2a** are close to those usually observed for LS iron(II) complexes. Owing to the fusion of five chelate rings, the shape of the [FeN_6] core noticeably deviates from the ideal octahedral geometry. The Fe–N distances are in the limits of 1.964(3)–2.047(3) Å (see Table 2) depending on the chemical nature of nitrogen atoms. The average Fe–N(pyridine) distance is shorter (1.987 Å) than the average Fe–N(aliphatic) one (2.012 Å). The shorter Fe–N(pyridine) distance is probably due to the π-back-bonding effect between the iron(II) atom and the pyridine rings. The N–Fe–N angles fall within the 80.3(1)–96.1(1)° range between the adjacent nitrogen atoms and 168.8(1)–174.7(1)° between the opposite ones (Table 2). The largest N–Fe–N deviation from 90° (80.3–87.4°) is observed in four sterically strained five-membered chelate rings. The presence of one six-membered chelate ring causes the release of some strain and the corresponding N2–Fe–N3 angle equals to 94.5(1)°. The six-membered chelate ring Fe-N2-C16-C17-C18-N3 adopts a *half-boat* conformation, which is also observed for **1a**.[27]

The relatively high anisotropic displacement parameter values for several fluorine atoms indicate a residual disorder in the counter-ion positions at 150 K. However, both BF_4 ions were resolved in a single orientation. The crystal packing of **1a** (Figure 7) and **2a** (Figure 8) are very similar and consist of alternate layers of molecules lying in the *bc* plane. Each layer involves two sheets with the antiparallel alignment of the molecules, which are related through the symmetry operation $-x$, $y+1/2$, $-z+1/2$. The molecules in a layer are strongly bound by H-bonding interactions through the B1 tetrafluoroborate anions inserted inside the layers. The B2 tetrafluoroborate anions arranged near the layer's border are less involved in the hydrogen-bonding interactions. The surface between the layers is filled by the carbon backbones of pyridine rings of the ligand. Several short intermolecular C···C contacts from partially π-stacked pyridine rings achieve the interlayer cohesion.

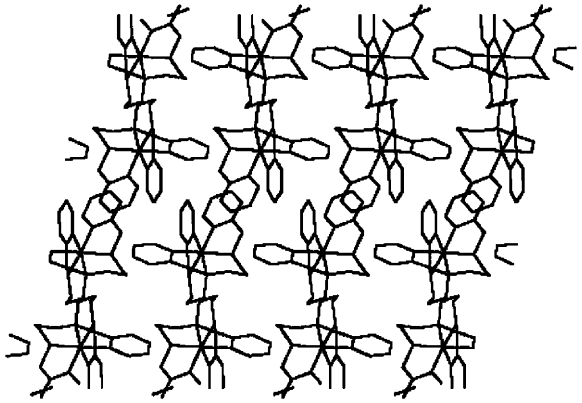

Figure 7. Projection of the molecular structure of [Fe(Hpy-DAPP)]$(BF_4)_2$ (**1a**) on the *ac* plane.

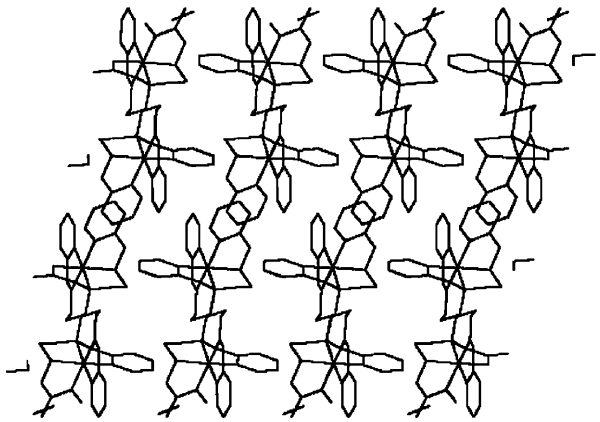

Figure 8. Projection of the molecular structure of [Fe(Hpy-EPPA)]$(BF_4)_2$ (**2a**) on the *ac* plane.

Low-spin 3a complex structure ($T=150$ K): The structural features for **3a** at 150 K are typical for iron(II) complexes with polydentate ligands in the LS state. The [FeN_6] polyhedron is not an ideal octahedron: the Fe–N distances vary in the limits of 1.973(2)–2.020(2) Å and the average Fe–N distance is equal to 1.991 Å. As in the case of **2a**, the average Fe–N(pyridine) distance in **3a** is shorter (1.977 Å) than the average Fe–N(aliphatic) one (2.004 Å). The N–Fe–N angles are also indicative for an octahedron with a certain degree of distortion (Table 2). The range of the N–Fe–N angles corresponds to 82.3(1)–96.9(1)° and 168.0(1)–174.0(1)°. Again as in **2a**, the largest N–Fe–N deviation from 90° (82.3–86.5°), as well as shortest N–N separations (2.634–2.756 Å), is found in five sterically strained five-membered chelate rings.

The crystal packing of **3a** (Figure 9) is similar to **1a** and **2a**. It can be also described as the alternation of layers along the *a* axis. Each layer consists of two sheets with the antiparallel alignment of the molecules related by the symmetry operation $-x$, $y+1/2$, $-z+1/2$. The molecules in the layers are strongly linked by the intermolecular H-bonding interactions through the fluorine atoms of the B1 tetrafluo-

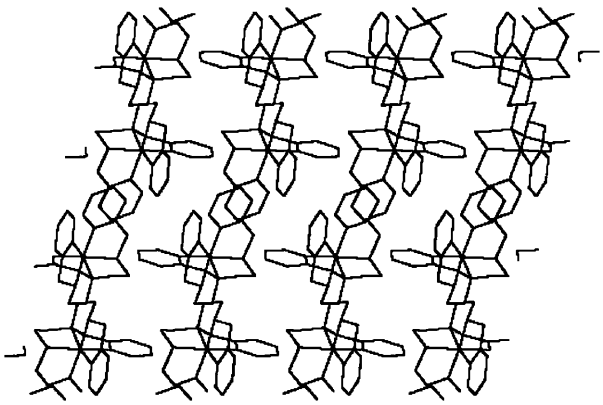

Figure 9. Projection of the molecular structure of [Fe(Hpy-DEPA)]$(BF_4)_2$ (**3a**) on the *ac* plane.

roborate anions incorporated inside the layers. The B2 tetrafluoroborate anions located near the layers periphery are less involved in the network of intermolecular H-bonds. The cohesion between the layers is ensured by several short intermolecular C···C contacts originated from partially π-stacked pyridine rings arranged within the layer's interface.

Discussion

The goal of the present work was to study the influence of strain effects, related to the size of chelate rings in the $[FeN_6]$ coordination sphere, on the spin-crossover characteristics within a family of related compounds. We previously attempted such a study with the iron(II) spin-crossover complexes with the two tetradentate ligands DPEA [(2-aminoethyl)bis(2-pyridylmethyl)amine][30] and DPPA [(3-aminopropyl)bis(2-pyridylmethyl)amine][25] through the enlargement of just one chelate ring from five- to six-membered. The two ligands differ by the presence of an additional methylene unit in the amino aliphatic chain of the DPPA ligand. However, the X-ray analysis revealed that, contrary to our expectation, the complexes $[Fe(DPEA)(NCS)_2]$ and $[Fe(DPPA)(NCS)_2]$ are the *mer* and *fac* stereoisomers, respectively, making a direct comparison of the metallocycle strain effects on magnetic properties irrelevant.

Being attracted by the tetradentate DAPP ([bis(3-aminopropyl)(2-pyridylmethyl)amine]) ligand ability to form a disordered six-membered chelate ring in the spin-crossover complex $[Fe(DAPP)(abpt)](ClO_4)_2$ (abpt = 4-amino-3,5-bis-(pyridin-2-yl)-1,2,4-triazole),[26] we synthesized on its base the hexadentate Hpy-DAPP ligand. The mononuclear complex **1a** with a two-step spin transition accompanied by ligand ordering in conjugation with a conformational transition was isolated.[27] In this work we present two more new ligands Hpy-EPPA and Hpy-DEPA. Together with Hpy-DAPP, they constitute a series of hexadentate ligands (Scheme 1) with the systematic change in the length of amino-aliphatic chains. All ligands are able to form five chelate rings with the iron(II) ion. Three chelate rings are similar in all complexes, whereas the amino-aliphatic chains of variable length yield two six-membered rings with Hpy-DAPP, one five- and one six-membered rings with Hpy-EPPA, and two five-membered rings with Hpy-DEPA. With each ligand, we synthesized three compounds $[Fe(L)]X_2$ with different counter ions ($X = BF_4$, PF_6, ClO_4). For convenience, we will refer to the corresponding complexes in the further discussion as (6,6) for **1a–c**, (6,5) for **2a–c**, and (5,5) for **3a–c**. Corroborating our expectation, the magnetic measurements, performed in the range of 15–500 K, have revealed that all compounds exhibit spin-crossover behavior. Remarkably, a striking regularity in the spin-transition temperatures has been found. Independently of the counter-ion nature, the rank of spin-transition temperatures is in direct relation with the chelate ring size. The transition temperatures of the compounds are ordered as $T_{1/2}$ (6,6) < $T_{1/2}$ (6,5) < $T_{1/2}$ (5,5). The X-ray structural studies have been performed for the three complexes with the BF_4 counter ion; although, as a result of high transition temperatures, only the LS structures have been determined for **2a** and **3a**. The analysis of three LS structures showed that the molecular cations correspond to the same stereoisomer and that the crystal packing is similar. One can hope that the same is true for the complexes with two other counter ions, PF_6 and ClO_4. So, the tendency of the spin-transition temperatures in this family of compounds can be entirely attributed to the influence of the strain effect, owed to the chelate rings size. This is the first clear example (to our knowledge) of the effect of the chelate rings size on the spin-transition temperature.

Several previous attempts to correlate the spin-transition temperature with the structural features of complexes have not led to an unambiguous structure–function relationship.[31] This can be explained, in part, by the relatively small number of structural data for the families of closely related compounds. It is expected that the spin-crossover temperature correlates with the ligand field strength. The aliphatic-nitrogen atoms included in the chelate rings, whose length is varied, act as σ-donors and their participation in π-bonding is negligible. The donor atoms belonging to five-membered rings donate more electronic density than those from six-membered rings, leading to an effective increase of the ligand field strength. This dependence is, for example, manifested in the electronic spectra of nickel(II)[18] and cobalt(III).[19–21] Although, this feature concerns σ-bonding, some effects from π-bonding also can not be excluded. The tilt of the pyridine rings, probably a result of packing effects, modifies the π-acceptor properties of the aromatic-nitrogen atoms. The comparison of the tilt angles of the pyridine rings from the coordination planes shows that they are rather close in **1a** and **2a** (10.5, 12.7, 9.9°, and 10.4, 14.9, 9.0°, respectively) compounds and slightly less in **3a** (10.0, 5.8, and 6.1°). However, the contribution of π-interactions in the ligand field strength is usually less important than that of σ-interactions.

We tried to analyze some structural characteristics of the family of compounds presented here, which may be related to the observed tendency of the spin-transition temperatures. If we focus on the averaged Fe–N distances, determining the ligand field force, they are equal to 2.061 Å, 2.000 Å, and 1.991 Å for **1a**, **2a**, and **3a**, respectively. It is easy to see that they are ordered as (5,5) < (5,6) < (6,6). Although, this order, corresponding to the ligand field weakening, concurs with the ordering of transition temperatures, the difference in the average bond lengths is too small to be convincing. However, if we look in more detail at the Fe–N bonds, we can observe that they are most dispersed for the (6,6) complex, and less dispersed for the (5,5). This indicates that the $[FeN_6]$ core in the latter is the most symmetric. The $[FeN_6]$ octahedron dissymmetry is more noticeable through the tetragonal distortion along the N2–Fe–N6 axis. The corresponding N2–N6 separations are found to be 4.179, 4.039, and 3.956 Å for **1a**, **2a**, and **3a**, respectively. This structural parameter is particularly important, owing to the fact that

the tertiary-amino aliphatic N2 atom is involved in both chelate rings of variable length. Another structural parameter, which is worth analyzing, is the trigonal twist angle. This idea arises from the work of Purcell,[32] who showed that the trigonal twist distortion of a d^6 octahedron could lead to a relative stabilization of the HS state and thus to a decrease of the spin-transition temperature. This distortion has been already suggested as a leading mechanism of the interconversion kinetics for several iron(II) complexes with hexadentate ligands.[22–24] If we consider two trigonal faces, as formed by the aliphatic- and aromatic-nitrogen atoms, the trigonal twist angles are found equal to 52.5, 50.7, and 50.3° for **1a**, **2a**, and **3a**, respectively, compared with 60° for a perfect octahedron. Not only is the difference between the twist-angle values very small, but also their sequence should lead to the transition temperatures order inverse to the values observed here. It seems that the trigonal twist does not enable us to explain the observed effects.

One of the ways to analyze internal strains that exist in the studied spin-crossover complexes can be based on the continuous shape measures intensively developed during last years by Avnir, Alvarez et al. and already applied in the research of structure–property correlations in spin crossover molecules.[28,29] This measure quantifies the deviation of a particular molecular polyhedron Q from an ideal highly-symmetric polyhedron P and is defined in Equation (1);

$$S_{\mathrm{Q}}(P) = \min\left[\frac{\sum_{i=1}^{N} |\vec{q}_i - \vec{p}_i|^2}{\sum_{i=1}^{N} |\vec{q}_i - \vec{q}_0|^2}\right] \times 100 \qquad (1)$$

In Equation (1), $\vec{q}_i$ are the Cartesian vectors of the vertices of the studied molecular polyhedron, with the center of mass at $\vec{q}_0$, and $\vec{p}_i$ are the vectors of the vertices of the ideal symmetric polyhedron characterized by a particular point symmetry group. The $S_Q(P)$ value can be ≤ 100 and equals to zero when the polyhedron Q has the shape of the polyhedron P. Two regular polyhedra should be studied for iron(II) hexacoordinated spin-crossover complexes, namely the octahedron (O_h symmetry) and the trigonal prism (D_{3h} symmetry). This choice is determined by two possible distortion pathways, which can lead to the crossing of singlet and quintet potential surfaces for d^6 complexes. One of them is a totally symmetric distortion of an octahedron, which is routinely analyzed in application to spin-crossover complexes (variation of Fe–N distances). The second one is a torsional distortion (trigonal Bailar twist), which can be represented as the relative motion of the two trigonal faces of an octahedron. We calculated $S(O_h)$ and $S(D_{3h})$ values (octahedricity and trigonal prismaticity) for three structurally studied complexes with the aid of the SHAPE program.[33] The results are presented in Figure 10. It can be seen that all polyhedra are rather close to a perfect octahedron, the $[FeN_6]$ core of the (5,5) complex is the most symmetrical. The trigonal prismaticity changes in the order $(5,5) < (5,6) < (6,6)$, meaning that the complex with the larger chelate ring deviates more,

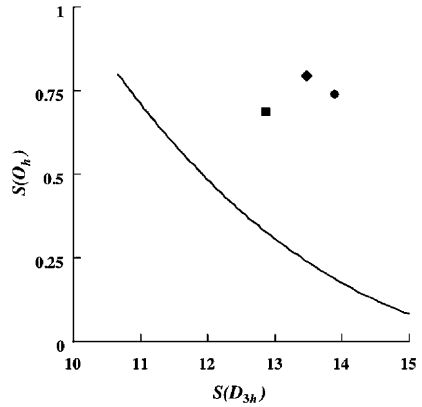

Figure 10. Octahedral and trigonal-prismatic shape measures for [Fe(Hpy-DAPP)]$(BF_4)_2$ (**1a**, ●), [Fe(Hpy-EPPA)]$(BF_4)_2$ (**2a**, ◆), [Fe(Hpy-DEPA)]$(BF_4)_2$ (**3a**, ■). The solid line corresponds to the Bailar twist for the interconversion of the octahedron and trigonal prism.

not only from an octahedron, but also from an ideal trigonal prism. Should the difference in the coordination core shapes to be comprised in the trigonal twist only, a proximity to trigonal prism symmetry would signify a relative stabilization of the HS state and, as a consequence, a lower spin-crossover temperature. The expected order of the points in Figure 10 would be (6,6), (5,6), and (5,5), going from left to right along the curve representing the Bailar twist. Our results give an inverse order. As the previous analysis of twist angles, the continuous shape measures approach confirms that the trigonal twist distortion cannot be considered as a structural feature beyond the spin-crossover temperature behavior. Going from (5,5) to (6,6) complex, we find a simultaneous increase of the octahedricity and trigonal prismaticity. It has been shown that such a dependence is characteristic for the Jahn–Teller type tetragonal distortion.[28] In our case, the tetragonal distortion is rather imposed by the size of chelate rings fused through the tertiary N2 nitrogen atom. It can be supposed that this particular feature plays a key role in the ordering of spin-transition temperatures. Notably, all previous analysis deals with the LS structural data only and further studies are necessary to get insight into both LS and HS structures. So far, we can mention that the geometries of the HS iron(II) complexes often display tetragonal distortions,[26] which, in this case, can be attributed to the Jahn–Teller (or, more exactly, pseudo-Jahn–Teller) effect. It can be a supplementary factor, enhancing the influence of tetragonal distortions.

Conclusion

In summary, we have synthesized a family of iron(II) complexes with hexadentate ligands, in which the size of chelate rings is systematically changed. All complexes, which possess a similar molecular and crystal structure, display the spin crossover phenomenon and, therefore, allow a direct study of the chelate-ring-size effects on the spin-transition

characteristics. The magnetic measurements unambiguously demonstrate that, independent of the nature of the counter ion, the expansion of the chelate ring results in the decrease of the transition temperature. These results pave the way to control the spin-crossover behavior of new systems.

Experimental Section

Chemistry: The syntheses were carried out in deoxygenated solvent under an inert atmosphere of N_2 by using glovebox techniques. *N*-(2-aminoethyl)-*N*-(3-aminopropyl)-2-(aminomethyl)pyridine (EPPA) and *N*,*N*-bis(2-aminoethyl)-2-(aminomethyl)pyridine (DEPA) were prepared according to a procedure previously reported.[34] The Hpy-DAPP ligand was synthesized by using the method described elsewhere.[27] The thermal stability of the samples of **3a** and **3b** compounds used in magnetic measurements was checked visually under microscope and through the IR spectroscopy. ^{1}H NMR spectra were recorded in $CDCl_3$ by using a Bruker AC200 spectrometer operating at 200 MHz.

Hpy-EPPA and Hpy-DEPA Ligands: A mixture of EPPA or DEPA (0.5 mmol) and 2-pyridinecarboxaldehyde (1 mmol) in methanol (15 mL) was refluxed under argon for 10 minutes. Then an excess of $NaBH_4$ (100 mg) was added in several small portions. The solution was allowed to stand overnight at room temperature and the solvent was evaporated under vacuum. After successive extraction of the crude product by $CHCl_3$ and Et_2O, the appropriate pure ligand was obtained as pale yellow oil. ^{1}H NMR ($CDCl_3$) for Hpy-EPPA: $\delta = 8.52$–7.06 (m, 12H; aromatic H's), 3.83–3.82 (d, 4H; CH_2), 3.70 (s, 2H; CH_2), 2.69–2.52 (m, 8H; CH_2), 1.83–1.68 ppm (m, 2H; CH_2; 2H; NH); ^{1}H NMR ($CDCl_3$) for Hpy-DEPA: $\delta = 8.47$–7.06 (m, 12H; aromatic H's), 3.82 (s, 4H; CH_2), 3.72 (s, 2H; CH_2), 2.71 (s, 8H; CH_2), 2.24 ppm (s, 2H; NH).

Preparation of the complexes: Compounds **2a** and **3a** were synthesized as follows: $FeCl_2 \cdot 2H_2O$ (0.15 mmol) was dissolved in ethanol/methanol (2 mL, 1:1 mixture) and NBu_4BF_4 (0.30 mmol) was added to it. After the addition of appropriate hexadentate ligand (0.15 mmol) in the same mixture of alcohols (2 mL), the solution turned dark red. The solution was filtered and allowed to stand overnight at room temperature to afford the crystals, which were collected by filtration, washed with ethanol, and dried in vacuum. The crystals used in the X-ray structure determination were selected from these samples.

[Fe(Hpy-EPPA)](BF$_4$)$_2$ (2a): Red-brown prismatic crystals. Elemental analysis calcd (%) for $C_{23}H_{30}N_6B_2F_8Fe$: C 44.56, H 4.88, N 13.56; found: C 44.81, H 4.47, N 13.67.

[Fe(Hpy-DEPA)](BF$_4$)$_2$ (3a): Dark-red plate crystals. Elemental analysis calcd (%) for $C_{22}H_{28}N_6B_2F_8Fe$: C 43.61, H 4.66, N 13.87; found: C 43.24, H 4.79, N 13.68.

Compounds **1b**, **2b**, and **3b** were prepared as follows: To a suspension of $FeCl_2 \cdot 2H_2O$ (0.15 mmol) and NBu_4PF_6 (0.30 mmol) in ethanol/methanol (2 mL, 1:1 mixture), an appropriate hexadentate ligand (0.15 mmol) in the same mixture of alcohols (2 mL) was added. The solution was filtered and allowed to stand overnight at room temperature, to afford the crystals, which were collected by filtration, washed with ethanol, and dried in vacuum.

[Fe(Hpy-DAPP)](PF$_6$)$_2$ (1b): Green-brown prismatic crystals. Elemental analysis calcd (%) for $C_{24}H_{32}N_6P_2F_{12}Fe$: C 38.42, H 4.30, N 11.20; found: C 37.95, H 4.17, N 11.47.

[Fe(Hpy-EPPA)](PF$_6$)$_2$ (2b): Red-brown prismatic crystals. Elemental analysis (%) calcd for $C_{23}H_{30}N_6P_2F_{12}Fe$: C 37.52, H 4.11, N 11.41; found: C 37.55, H 4.20, N 11.06.

[Fe(Hpy-DEPA)](PF$_6$)$_2$ (3b): Dark-red prismatic crystals. Elemental analysis calcd (%) for $C_{22}H_{28}N_6P_2F_{12}Fe$: C 36.58, H 3.91, N 11.64; found: C 36.73, H 3.67, N 11.35.

Complexes **1c**, **2c**, and **3c** were synthesized according to following procedure: To a solution of $Fe(ClO_4)_2 \cdot 6H_2O$ (0.15 mmol) in methanol (1 mL), a solution of the ligand (0.15 mmol) in methanol/ethanol (2 mL, 1:1 mixture) was added dropwise. The solution was filtered and allowed to stand overnight at room temperature to give the crystals, which were collected by filtration, washed with ethanol and dried under vacuum.

[Fe(Hpy-DAPP)](ClO$_4$)$_2$ (1c): Green-plate crystals. Elemental analysis calcd (%) for $C_{24}H_{32}N_6Cl_2O_8Fe$: C 43.72, H 4.78, N 12.75; found: C 43.33, H 4.51, N 13.06.

[Fe(Hpy-EPPA)](ClO$_4$)$_2$ (2c): Brown-needle crystals. Elemental analysis calcd (%) for $C_{23}H_{30}N_6Cl_2O_8Fe$: C 42.81, H 4.69, N 13.02; found: C 42.67, H 4.35, N 13.29.

[Fe(Hpy-DEPA)](ClO$_4$)$_2$ (3c): Brown-needle crystals. Elemental analysis calcd (%) for $C_{22}H_{28}N_6Cl_2O_8Fe$: C 41.86, H 4.47, N 13.31; found: C 41.57, H 4.62, N 13.09.

CAUTION: Perchlorate salts of metals with organic ligands are potentially explosive. Only small quantities of the compound should be prepared and handled with much care!

Physical measurements

Magnetic properties: Magnetic susceptibility measurements were carried out in the temperature range 15–500 K by using a fully automated Manics DSM-10 susceptometer equipped with a TBT continuous cryostat and an electromagnet operating at 1.6 Tesla. Data were corrected for diamagnetic contributions.

Solution and refinement of the X-ray structure: Suitable Crystals were selected and mounted on a Nonius Kappa CCD diffractometer ($Mo_{K\lambda}$ radiation, $\lambda = 0.71073$ Å). Intensities were collected at 150 K by means of the COLLECT software.[35] Reflection indexing, Lorentz-polarization correction, peak integration and background determination were carried out with DENZO.[36] Frame scaling and unit-cell parameters refinement were made with SCALEPACK.[36] An analytical absorption correction was applied using the modeled faces of the crystal.[37] The structures were solved by direct methods with SIR97.[38] The remaining non-hydrogen atoms were located by successive difference Fourier map analyses. The hydrogen atoms were placed geometrically and included in the refinement using soft restraints on the bond lengths and angles to regularize their geometry (C-H in the range 0.93–0.98 Å and N-H in the range 0.86–0.89 Å) and isotropic atomic displacement parameters (U(H) in the range 1.2–1.5 times $U_{eq.}$ of the adjacent atom). In the last cycles of the refinement, the hydrogen atoms were refined using a riding mode. The structure refinement was carried out with CRYSTALS.[39]

CCDC 700957 (**3a**), and 700958 (**2a**) contain the supplementary crystallographic data for this paper. These data can be obtained free of charge from The Cambridge Crystallographic Data Centre via www.ccdc.cam.ac.uk/data_request/cif.

Acknowledgement

We are grateful to the Region Rhône–Alpes for a grant to M.B.B. The authors are thankful to S. Alvarez and M. Llunell for providing the SHAPE program. We are grateful to the referee for valuable remarks. This work was supported by the EU through NE MAGMANET (FP6-NMP3-CT-2005–515767).

[1] L. Cambi, L. Szegö, *Ber. Dtsch. Chem. Ges.* **1931**, *64*, 2591–2598.
[2] O. Kahn, *Molecular Magnetism*, Wiley-VCH, **1993**.
[3] The main early research is summarized in: *Topics in Current Chemistry, Vols. 233–235* (Eds.: P. Gütlich, H. A. Goodwin), Springer, **2004**.
[4] A. Bousseksou, G. Molnàr, G. S. Matouzenko, *Eur. J. Inorg. Chem.* **2004**, 4353–4369.
[5] P. Gütlich, P. J. van Koningsbruggen, F. Renz, *Struct. Bonding (Berlin)* **2004**, *107*, 27–75.
[6] A. B. Gaspar, V. Ksenofontov, M. Seredynyuk, P. Gütlich, *Coord. Chem. Rev.* **2005**, *249*, 2661–2676.
[7] J. A. Real, A. B. Gaspar, M. C. Muñoz, *Dalton Trans.* **2005**, 2062–2079.

[8] M. Sorai, M. Nakano, Y. Miyazaki, *Chem. Rev.* **2006**, *106*, 976–1031.
[9] A. Bousseksou, G. Molnár, J. A. Real, K. Tanaka, *Coord. Chem. Rev.* **2007**, *251*, 1822–1833.
[10] M. A. Halcrow, *Polyhedron* **2007**, *26*, 3523–3576.
[11] K. S. Murray, *Eur. J. Inorg. Chem.* **2008**, 3101–3121.
[12] O. Kahn, J.-P. Launay, *Chemtronics* **1988**, *3*, 140–144.
[13] O. Kahn, J. Kröber, C. Jay, *Adv. Mater.* **1992**, *4*, 718–728.
[14] B. M. T. Lam, J. A. Halfen, V. G. Young, Jr., J. R. Hagadorn, P. L. Holland, A. Lledos, L. Cucurull-Sanchez, J. J. Novoa, S. Alvarez, W. B. Tolman, *Inorg. Chem.* **2000**, *39*, 4059–4072.
[15] M. Schatz, M. Becker, F. Thaler, F. Hampel, S. Schindler, R. R. Jacobson, Z. Tyeklar, N. N. Murthy, P. Ghosh, Q. Chen, K. D. Karlin, *Inorg. Chem.* **2001**, *40*, 2312–2322.
[16] M. Merkel, M. Pascaly, B. Krebs, J. Astner, S. P. Foxon, S. Schindler, *Inorg. Chem.* **2005**, *44*, 7582–7589.
[17] Y. Gultneh, T. B. Yisgedu, Y. T. Tesema, R. J. Butcher, *Inorg. Chem.* **2003**, *42*, 1857–1867.
[18] C. Ochs, F. E. Hahn, T. Lügger, *Eur. J. Inorg. Chem.* **2001**, 1279–1285.
[19] P. M. Jaffray, L. F. McClintock, K. E. Baxter, A. G. Blackman, *Inorg. Chem.* **2005**, *44*, 4215–4225.
[20] G. Cavigliasso, R. Stranger, L. F. McClintock, S. Cheyne, P. M. Jaffray, K. E. Baxter, A. G. Blackman, *Dalton Trans.* **2008**, 2433–2441.
[21] C. A. Jiménez, J. B. Belmar, J. Alderete, F. S. Delgado, M. Lopez-Rodriguez, O. Peña, M. Julve, C. Ruiz-Perez, *Dalton Trans.* **2007**, 2135–2144.
[22] H. R. Chang, J. K. McCusker, H. Toftlund, S. R. Wilson, A. X. Trautwein, H. Winkler, D. N. Hendrickson, *J. Am. Chem. Soc.* **1990**, *112*, 6814- 6827.
[23] J. K. McCusker, A. L. Rheingold, D. N. Hendrickson, *Inorg. Chem.* **1996**, *35*, 2100–2112.
[24] L. Christiansen, D. N. Hendrickson, H. Toftlund, S. R. Wilson, C.-L. Xie, *Inorg. Chem.* **1986**, *25*, 2813–2818.
[25] G. S. Matouzenko, A. Bousseksou, S. Lecocq, P. J. van Koningsbruggen, M. Perrin, O. Kahn, A. Collet, *Inorg. Chem.* **1997**, *36*, 5869–5879.
[26] G. S. Matouzenko, A. Bousseksou, S. A. Borshch, M. Perrin, S. Zein, L. Salmon, G. Molnàr, S. Lecocq, *Inorg. Chem.* **2004**, *43*, 227–236.
[27] G. S. Matouzenko, D. Luneau, G. Molnar, N. Ould-Moussa, S. Zein, S. A. Borshch, A. Bousseksou, F. Averseng, *Eur. J. Inorg.* Chem. **2006**, 2671–2682.
[28] S. Alvarez, D. Avnir, M. Llunell, M. Pinsky, *New J. Chem.* **2002**, *26*, 996–1009.
[29] S. Alvarez, *J. Am. Chem. Soc.* **2003**, *125*, 6795–6802.
[30] G. S. Matouzenko, A. Bousseksou, S. Lecocq, P. J. van Koningsbruggen, M. Perrin, O. Kahn, A. Collet, *Inorg. Chem.* **1997**, *36*, 2975–2981.
[31] P. Guionneau, M. Marchivie, G. Bravic, J.-F. Létard, D. Chasseau, *Topics in Current Chemistry, Vol. 234* (Eds. : P. Gütlich, H. A. Goodwin), Springer, **2004**, p. 97–128.
[32] K. Purcell, *J. Am. Chem. Soc.* **1979**, *101*, 5147–5152.
[33] M. Llunell, D. Casanova, J. Cirera, J. M. Bofill, P. Alemany, S. Alvarez, M. Pinsky, D. Avnir, SHAPE (1.1b); Barcelona, **2003**.
[34] M. B. Bushuev, E. Jeanneau, D. Luneau, G. S. Matouzenko, *Inorg. Chim. Acta* **2007**, *360*, 1639–1644.
[35] Nonius, *COLLECT*, Nonius B. V., Delft, The Netherlands, **1997–2001**.
[36] Z. Otwinowski, W. Minor, *Methods Enzymol.* **1997**, *276*, 307–326.
[37] J. de Meulenaer, H. Tompa, *Acta Crystallogr. Sect.* **1965**, *A19*, 1014–1018.
[38] A. Altomare, M. C. Burla, M. Camalli, G. L. Cascarano, C. Giacovazzo, A. Guagliardi, A. G. G. Moliterni, G. Polidori and R. Spagna, *J. Appl. Crystallogr.* **1999**, *32*, 115–119.
[39] P. W. Betteridge, J. R. Carruthers, R. I. Cooper, K. Prout and D. J. Watkin, *J. Appl. Crystallogr.* **2003**, *36*, 1487.

Received: September 29, 2008
Published online: December 16, 2008

